韓國鑛物學會誌 第 11 卷 第 2 號 (1998)
J. Miner. Soc. Korea, 11, 69-84 (1998)

# Mineralogical Study of Sericite in the Daehyun Mine: Formation, Chemistry and Polytype

## 대현광산 견운모의 생성과정과 화학조성 및 폴리타잎

Byung Ym Rhee (이병임) · Soo Jin Kim (김수진)

Department of Geological Science, Seoul National University, Seoul 151-742, Korea
(서울대학교 지질과학과)

**ABSTRACT** : The Daehyun sericite deposit in Socheon-myun, Bongwha-gun, Kyungsangbuk-do, Korea, has been formed by the hydrothermal alteration of the Hongjesa granite of Precambrian age, leaving the muscovite granite between ore body and the Hongjesa granite as the wall rock alteration zone. The process of sericitization of granitic rock as well as the chemistry and structures of sericites were studied using polarizing microscope, X-ray diffractometer (XRD), electron probe microanalyzer (EPMA) and high resolution transmission electron microscope (HRTEM). There are two genetic types of sericites having different chemistry and structure. The early sericite is of $2M_1$ polytype and has octahedral composition close to muscovite. It has been formed from the primary muscovite, tourmaline and quartz under a relatively high temperature. The late sericite is of 1M, $2M_1$ and 3T polytypes and has phengitic composition. It has been formed from feldspar, biotite, muscovite and tourmaline under a relatively low temperature. Chemical analyses show that the early sericite has less $Mg+Fe_T$ content and lower $Si/Al^{IV}$ ratio in tetrahedral site than the late sericite.

요약 : 경북 봉화군 소천면에 위치하는 대현광산의 견운모는 모암인 홍제사 화강암이 열수변질을 받아 생성되었으며 그 과정 중에 생성된 백운모화강암이 광체와 모암 사이에 모암변질대로 발견된다. 본 연구에서는 이 지역 견운모의 생성과정과 화학조성 및 구조를 연구하였으며, 이를 위하여 편광현미경, X-선분말회절기, 주사전자현미경, 전자현미분석기와 고해상투과전자현미경 등 기기들이 사용되었다. 그 결과 대현광산 견운모의 화학조성과 구조는 그 생성시기와 관련하여 두 타입으로 나누어진다. 먼저 생성된 견운모는 백운모에 가까운 8면체조성과 $2M_1$ 폴리타잎을 가지며 비교적 고온환경에서 1차 백운모와 전기석, 석영으로부터 생성된 반면, 나중에 생성된 견운모는 펜자이트에 가까운 조성과 1M, $2M_1$, 3T의 폴리타잎을 가지며 비교적 저온환경에서 장석, 흑운모, 백운모, 전기석으로부터 생성되었다. 전자는 후자에 비해 $Mg+Fe_T$ 함량이 적으며 4면체조성의 $Si/Al^{IV}$ 비율도 낮다.

## INTRODUCTION

A lot of metallic minerals have been used in industry, but recently the demand for the nonmetallic minerals are very rapidly increasing. Non-metallic minerals including clays are used for raw materials in ceramic and allied industries. Among them sericite attracts our parti

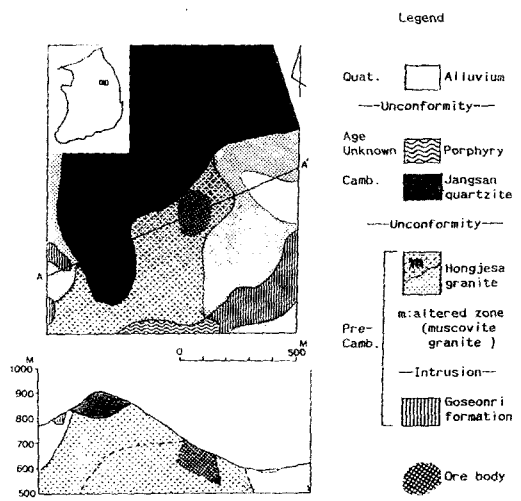


**Fig. 1.** Geological map and cross section of the Daehyun mining area, Korea.

cular attention because of its use for alkali flux (Robinson, 1984) and cosmetics (Tokubo, 1986; 양정일 외, 1996).

The Daehyun sericite deposit is located in Daehyun 3-ri, Socheon-myun, Bongwha-gun, Kyungsangbuk-do (Lat. 37° 3′ 30″ N, and Long. 129° E), Korea (Fig. 1). It occupies the southwestern part of the Precambrian Hongjesa granite in contact with the Paleozoic Jangsan quartzite.

Sericite from the Daehyun mine is generally of high quality containing only small amounts of muscovite and quartz. It is a hydrothermal product which has been formed by the interaction of the host Hongjesa granite and later hydrothermal solution. During this alteration most of constituent minerals of the Hongjesa granite, including quartz and tourmaline, have been sericitized.

The present paper aims to study the processes of sericitization of granitic rock with emphasis on the chemistry and structure of sericites.

## GEOLOGICAL SETTING

Geology of the Daehyun mining area consists of the Goseonri Formation and the Hongjesa grante of Precambrian age, the Jangsan quartzite of Cambrian age and porphyry of age-unknown. Geological map and cross section of the Daehyun mining area are shown in Fig. 1. The Hongjesa granite, the host rock of sericite ore deposit, has been altered to the muscovite granite as shown in the geological map. The muscovite granite has been regarded as a later intrusion after the Honjesa granite by Kim et al. (1984) who called it leucocratic muscovite granite. But Rhee (1991) proposed that the muscovite granite in the Daehyun mine is a hydrothermal alteration product of the Hongjesa granite. It, therefore, is expected that sericite ore body is embedded in the muscovite granite in large scale as shown in the cross section (Fig. 1).

The sericite has 202.5±4.53 Ma. by K-Ar age dating (Park et al., 1988). Many workers (Kim et al., 1978; KIER, 1984; KMPC, 1987) have studied the geology and petrography of the Hongjesa granite. But detailed mineralogical study has not been made yet.

## EXPERIMENTAL

Chemical analyses of rocks were carried out using Perkin Elmmer atomic absorption spectrometer (AA) model 703. CIPW norm was obtained by the computer program MAIN designed for the IBM PC. Chemical analyses of minerals were made using a JEOL electron probe microanalyzer (EPMA) model JXA-733 attached with LINK AN 10000 energy dispersive spectrometer.

Identification of minerals were done using a Rigaku X-ray powder diffractometer (XRD) model RAD 3-C with Ni-filtered CuK$\alpha$ radiation. X-ray data were used to detect the variation of mineral compositions with the increasing alteration of the host rock, and to identify polytypes of sericites.

High resolution transmission electron microscope (HRTEM) was used for structural analysis through the electron diffraction pattern and the lattice fringe images. Specimens were examined at 200KV with a JEOL JEM-2000EX instrument.

**Table 1.** Chemical analyses and C.I.P.W. norms of the Hongjesa granite and the muscovite granite.

| | Hongjesa granite | | | | Muscovite granite | | |
|---|---|---|---|---|---|---|---|
| # | 8A5-3 | 8A6 | 8A7 | 38B | 8D1 | 8E1 | 7-46 |
| $SiO_2$ | 68.10 | 69.80 | 66.20 | 65.20 | 72.50 | 72.20 | 72.80 |
| $TiO_2$ | 0.39 | 0.37 | 0.51 | 0.73 | 0.08 | 0.13 | 0.06 |
| $Al_2O_3$ | 15.00 | 12.90 | 15.90 | 16.60 | 12.50 | 12.70 | 13.50 |
| $Cr_2O_3$ | 0.00 | 0.00 | 0.01 | 0.01 | 0.00 | 0.01 | 0.00 |
| $Fe_2O_3$ | 1.00 | 0.94 | 1.22 | 1.71 | 0.11 | 0.17 | 0.12 |
| FeO | 2.16 | 2.60 | 4.04 | 2.41 | 1.08 | 1.08 | 0.29 |
| MnO | 0.03 | 0.06 | 0.07 | 0.06 | 0.03 | 0.02 | 0.01 |
| MgO | 1.19 | 1.33 | 1.66 | 1.24 | 0.47 | 0.44 | 0.14 |
| CaO | 0.38 | 1.35 | 1.44 | 1.16 | 0.78 | 0.34 | 0.34 |
| $Na_2O$ | 4.07 | 4.31 | 4.38 | 5.11 | 2.31 | 2.63 | 3.43 |
| $K_2O$ | 3.47 | 2.72 | 3.17 | 2.84 | 6.05 | 6.69 | 6.42 |
| $B_2O_3$ | 0.01 | 0.18 | 0.08 | 0.02 | 0.06 | 0.01 | 0.05 |
| Total | 95.80 | 96.56 | 98.68 | 97.09 | 95.97 | 96.42 | 97.16 |
| C.I.P.W. Norm, Vol % | | | | | | | |
| Q | 27.39 | 27.86 | 20.43 | 19.10 | 32.71 | 29.16 | 27.18 |
| C | 3.86 | 0.41 | 2.65 | 3.01 | 0.73 | 0.51 | 0.29 |
| Or | 20.51 | 16.08 | 18.76 | 16.78 | 35.75 | 39.54 | 37.94 |
| Ab | 34.44 | 36.47 | 37.06 | 43.24 | 19.55 | 22.26 | 29.03 |
| An | 1.89 | 6.70 | 7.14 | 5.76 | 3.87 | 1.69 | 1.69 |
| HyEn | 2.96 | 3.31 | 4.14 | 3.09 | 1.17 | 1.10 | 0.35 |
| HyFs | 2.55 | 3.50 | 5.69 | 2.57 | 1.81 | 1.66 | 0.35 |
| Mt | 1.45 | 1.36 | 1.77 | 2.48 | 0.16 | 0.25 | 0.17 |
| Il | 0.74 | 0.70 | 0.97 | 0.63 | 0.15 | 0.25 | 0.11 |
| Ch | 0.01 | 0.01 | 0.01 | 0.01 | 0.00 | 0.01 | 0.00 |
| Total | 95.80 | 96.40 | 98.63 | 96.67 | 95.91 | 96.41 | 97.11 |

Q : quartz, C : corundum, Or : orthoclase, Ab : albite, An : anorthite,
HyEn : enstatite, HyFs : ferrosilite, Mt : magnetite, Il : ilmenite, Ch : chromite.

**Table 2.** Electron microprobe analyses of muscovite in the Daehyun mine.

| | Primary muscovite | | | | Secondary muscovite | | | |
|---|---|---|---|---|---|---|---|---|
| | Hongjesa gr. | | Muscovite gr. | | Muscovite gr. | | | |
| # | 5-2-3 | 8A6-3 | A3-22 | D1-54 | A3-7 | A3-14 | D1-15 | E3-38 |
| $SiO_2$ | 44.86 | 45.33 | 45.67 | 45.88 | 47.21 | 48.39 | 46.70 | 48.101 |
| $TiO_2$ | 0.37 | 0.52 | 0.52 | 0.09 | 0.01 | 0.10 | 0.09 | 0.20 |
| $Al_2O_3$ | 35.88 | 34.84 | 35.10 | 35.28 | 28.46 | 29.23 | 30.13 | 28.04 |
| $Cr_2O_3$ | 0.00 | 0.00 | 0.00 | 0.00 | 0.04 | 0.07 | 0.00 | 0.00 |
| FeO* | 0.97 | 1.45 | 1.32 | 1.61 | 4.24 | 3.53 | 3.77 | 3.33 |
| MgO | 0.55 | 0.89 | 0.92 | 0.80 | 2.50 | 2.69 | 2.34 | 2.37 |
| MnO | 0.03 | 0.10 | 0.00 | 0.01 | 0.07 | 0.10 | 0.00 | 0.01 |
| CaO | 0.00 | 0.00 | 0.00 | 0.00 | 0.04 | 0.01 | 0.01 | 0.01 |
| $Na_2O$ | 0.66 | 0.39 | 0.46 | 0.34 | 0.09 | 0.07 | 0.09 | 0.09 |
| $K_2O$ | 10.05 | 10.75 | 10.74 | 11.02 | 10.66 | 11.26 | 10.10 | 11.08 |
| Total | 93.37 | 94.27 | 94.73 | 95.03 | 93.40 | 95.44 | 93.24 | 93.24 |
| Numbers of ions on the basis of 22 oxygens | | | | | | | | |
| Si | 6.077 | 6.122 | 6.129 | 6.148 | 6.525 | 6.532 | 6.422 | 6.632 |
| $Al^{IV}$ | 1.923 | 1.878 | 1.871 | 1.852 | 1.475 | 1.468 | 1.578 | 1.368 |
| Tet. | 8.000 | 8.000 | 8.000 | 8.000 | 8.000 | 8.000 | 8.000 | 8.000 |
| $Al^{VI}$ | 3.805 | 3.668 | 3.680 | 3.720 | 3.160 | 3.182 | 3.305 | 3.187 |
| Ti | 0.037 | 0.053 | 0.052 | 0.009 | 0.009 | 0.010 | 0.009 | 0.021 |
| Cr | 0.000 | 0.000 | 0.000 | 0.000 | 0.005 | 0.008 | 0.000 | 0.000 |
| Fe | 0.110 | 0.164 | 0.148 | 0.181 | 0.490 | 0.398 | 0.433 | 0.384 |
| Mg | 0.110 | 0.179 | 0.183 | 0.160 | 0.515 | 0.541 | 0.480 | 0.488 |
| Mn | 0.004 | 0.011 | 0.000 | 0.001 | 0.008 | 0.012 | 0.000 | 0.002 |
| Oct. | 4.066 | 4.075 | 4.064 | 4.071 | 4.187 | 4.150 | 4.228 | 4.081 |
| Ca | 0.000 | 0.000 | 0.000 | 0.000 | 0.007 | 0.001 | 0.001 | 0.002 |
| Na | 0.173 | 0.102 | 0.119 | 0.087 | 0.025 | 0.018 | 0.025 | 0.024 |
| K | 1.737 | 1.852 | 1.839 | 1.883 | 1.879 | 1.938 | 1.772 | 1.949 |
| Int. | 1.911 | 1.954 | 1.958 | 1.971 | 1.911 | 1.957 | 1.798 | 1.974 |
| Ch(Tet) | -1.92 | -1.88 | -1.87 | -1.85 | -1.48 | -1.47 | -1.58 | -1.37 |
| Ch(Oct) | 0.01 | -0.08 | -0.09 | -0.12 | -0.44 | -0.49 | -0.22 | -0.61 |
| Ch(Int) | 1.91 | 1.95 | 1.96 | 1.97 | 1.92 | 1.96 | 1.80 | 1.98 |
| $Si/Al^{IV}$ | 3.161 | 3.260 | 3.276 | 3.320 | 4.423 | 4.450 | 4.069 | 4.847 |
| Na/Na+K | 0.091 | 0.052 | 0.061 | 0.044 | 0.013 | 0.009 | 0.014 | 0.012 |
| Mg/Fe+Mg | 0.501 | 0.521 | 0.553 | 0.470 | 0.512 | 0.576 | 0.525 | 0.559 |

*Total Fe as FeO.

**Table 3.** Electron microprobe analyses of feldspars in the Hongjesa granite and the muscovite granite.

| | Hongjesa granite | | | | Muscovite granite | | | |
|---|---|---|---|---|---|---|---|---|
| | plagioclase | | K-feldspar | | plagioclase | | K-feldspar | |
| # | A6-10 | A7-6 | A6-4 | A7-24 | 5-3-2 | D1-44 | A4-18 | D1-52 |
| $SiO_2$ | 61.69 | 62.35 | 64.06 | 62.05 | 68.08 | 66.46 | 62.73 | 63.51 |
| $TiO_2$ | 0.04 | 0.03 | 0.04 | 0.02 | 0.00 | 0.00 | 0.00 | 0.00 |
| $Al_2O3$ | 24.80 | 22.96 | 19.12 | 18.26 | 20.06 | 20.66 | 18.82 | 18.47 |
| $Cr_2O_3$ | 0.00 | 0.06 | 0.00 | 0.01 | 0.02 | 0.00 | 0.02 | 0.00 |
| $Fe_2O_3$ * | 0.04 | 0.09 | 0.05 | 0.01 | 0.03 | 0.04 | 0.00 | 0.02 |
| MgO | 0.00 | 0.00 | 0.01 | 0.00 | 0.00 | 0.00 | 0.01 | 0.00 |
| MnO | 0.08 | 0.00 | 0.11 | 0.00 | 0.07 | 0.00 | 0.00 | 0.00 |
| CaO | 3.87 | 3.69 | 0.00 | 0.00 | 0.05 | 0.85 | 0.03 | 0.00 |
| $Na_2O$ | 9.32 | 9.76 | 0.61 | 0.36 | 11.89 | 11.59 | 0.40 | 0.48 |
| $K_2O$ | 0.13 | 0.21 | 15.54 | 14.74 | 0.05 | 0.06 | 16.20 | 16.06 |
| Total | 99.97 | 99.14 | 99.54 | 95.46 | 100.24 | 99.66 | 98.21 | 98.55 |
| Numbers of ions on the basis of 8 oxygens | | | | | | | | |
| Si | 2.732 | 2.786 | 2.968 | 2.987 | 2.971 | 2.927 | 2.960 | 2.982 |
| Al | 1.294 | 1.209 | 1.044 | 1.036 | 1.032 | 1.072 | 1.047 | 1.022 |
| Total | 4.026 | 3.995 | 4.012 | 4.023 | 4.002 | 3.999 | 4.007 | 4.004 |
| Ti | 0.001 | 0.001 | 0.001 | 0.001 | 0.000 | 0.000 | 0.000 | 0.000 |
| Cr | 0.000 | 0.002 | 0.000 | 0.000 | 0.001 | 0.000 | 0.001 | 0.000 |
| Fe | 0.001 | 0.003 | 0.002 | 0.000 | 0.001 | 0.001 | 0.000 | 0.001 |
| Mg | 0.000 | 0.000 | 0.001 | 0.000 | 0.000 | 0.000 | 0.001 | 0.000 |
| Mn | 0.003 | 0.000 | 0.004 | 0.000 | 0.002 | 0.000 | 0.000 | 0.000 |
| Ca | 0.184 | 0.177 | 0.000 | 0.000 | 0.002 | 0.040 | 0.001 | 0.000 |
| Na | 0.800 | 0.846 | 0.055 | 0.034 | 1.006 | 0.989 | 0.036 | 0.044 |
| K | 0.007 | 0.012 | 0.919 | 0.905 | 0.003 | 0.003 | 0.975 | 0.962 |
| Total | 0.997 | 1.040 | 0.982 | 0.941 | 1.015 | 1.034 | 1.015 | 1.006 |
| Mole% | | | | | | | | |
| An | 18.5 | 17.1 | 0.1 | 0.0 | 0.2 | 3.9 | 0.2 | 0.0 |
| Ab | 80.7 | 81.8 | 5.7 | 3.6 | 99.5 | 95.8 | 3.6 | 4.4 |
| Or | 0.7 | 1.1 | 94.3 | 96.4 | 0.3 | 0.3 | 96.2 | 95.6 |

An : Ca+Mg, Ab : Na, Or : K.

* Total Fe as $Fe_2O_3$.

## PETROGRAPHY AND PETROCHEMISTRY OF HOST ROCK

The Hongjesa granite, the host rock of the Daehyun sericite deposit, has medium - to coarse - grained granular texture with partial porphyritic texture. It consists mainly of quartz, plagioclase, microcline, biotite and muscovite with minor chlorite, tourmaline, zircon, apatite, etc.

The Hongjesa granite was hydrothermally altered to the muscovite granite, thus the contact of both rocks is gradational. They have the same texture but have different mineralogical composition. Especially the contents of mica and the composition of plagioclase are characteristic for both rocks.

Table 1 represents whole rock chemical analyses and CIPW norm for the Hongjesa granite and the muscovite granite. The computer program MAIN designed for the IBM PC is used for calculating CIPW norm on the basis of the procedure suggested by Kelsie (1965). According to Table 1, the muscovite granite contains higher $SiO_2$ and $K_2O$ contents compared with the Hongjesa granite, but the chemical trends of other oxides show regressive variations from the Hongjesa granite to the muscovite granite. This phenomenon is mainly due to the alteration of mica and plagioclase.

The unaltered Hongjesa granite contains abundant biotite (5.5%) and small amount of muscovite (2.8%). But the muscovite granite is leucocratic because of the alteration of biotite to muscovite. Therefore two kinds of muscovite (12.4%) are found in the deposit : one is the primary muscovite and the other is the secondary hydrothermal muscovite which has formed from biotite by alteration. The secondary muscovite has higher $Si/Al^{IV}$ ratio and higher $Mg+Fe_T$ content, but lower Na/(Na+K) ratio compared with the primary one (Table 2).

Chemical analyses show that plagioclases in both rocks have different compositions to each other (Table 3). Table 3 shows the only several selected ones. Plagioclases (17.8%) contained in the Hongjesa granite largely belong to oligoclase with the composition of $Ab_{78-84}$. They are commonly replaced by K-feldspar. Some plagioclases have been already partially altered to sericites, which might be the incipient alteration products formed during the last solidifying stage. Such sericites are extremely fine-grained and fragile. On the contrary, plagioclases (15.5%) in the muscovite granite belong to albite with the composition of $Ab_{95-100}$, and have been fairly sericitized. In the transition zone between the two rocks, both oligoclase and albite are present together, indicating that the muscovite granite might be the hydrothermal alteration product of the Hongjesa granite.

Microcline (22.1%) contained in the Hongjesa granite has the composition of $Or_{94-96}Ab_{4-6}$ (Table 3), and sometimes occurs as an anhedral phenocryst. It generally shows fresh grid twin, but partly perthitic texture. Albite blebs are of string or irregular patch type. Microcline (29.2%) in the muscovite granite, even though it was partly altered, also shows a grid twin and perthitic texture. It has the composition of $Or_{95-98}Ab_{2-5}$, suggesting that it approaches Or end member. Chlorite is mainly observed in the host rock as the alteration product of micas. Chlorite in the study area largely corresponds to the variety ripidolite. Quartz occurs not only as one of the original constituent minerals of the Hongjesa granite but also as the secondary product. Quartz occasionally shows wavy extinction and inclusion zoning. Myrmekitic intergrowth of quartz is often observed within plagioclase along the contact with microcline, and occasionally associated with tourmaline. The characteristic microscopic texture of quartz containing rutile is found in both rocks, suggesting that the muscovite granite is the alteration product of the Hongjesa granite. Tourmaline occurring as an accessory mineral belongs to the draviteschorl series.

## SERICITE MINERALIZATION

Sericite deposit is developed as a big oblate body having the size of $140 \times 200$ m$^2$ in the muscovite granite which has been formed from the Hongjesa granite by hydrothermal alteration related to the sericite mineralization. Gradational contacts between the sericite ore body and the muscovite granite and between the muscovite granite and the unaltered Hongjesa granite suggest that the sericite body is the highly altered zone and the muscovite granite is the less altered zone.

Fig. 2 shows the photomicrographs of unaltered Hongjesa granite, the moderately altered rock and the sericite ore. The original minerals and textures of the Hongjesa granite have been completely destroyed producing new very fine-grained textures of sericite ore. Quartz or quartz-tourmaline veinlets are found in the sericite ore body. X-ray diffraction analyses of a series of rocks (Fig. 3) from the host rock to the sericite ore body show that sericite was formed at the expense of constituent minerals of the Hongjesa granite.

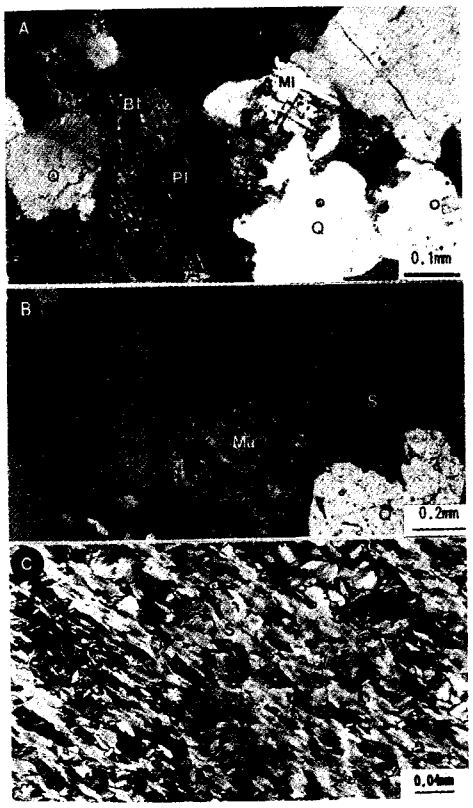


**Fig. 2.** Photomicrographs showing the gradational sericitization from the host rock to sericite. Crossed nicols (Bt; biotite, Pl; plagioclase, Mi; microcline, Q; quartz, Mu; muscovite, S; sericite). A: Host rock, B: Moderately altered rock, C: Completely altered rock.

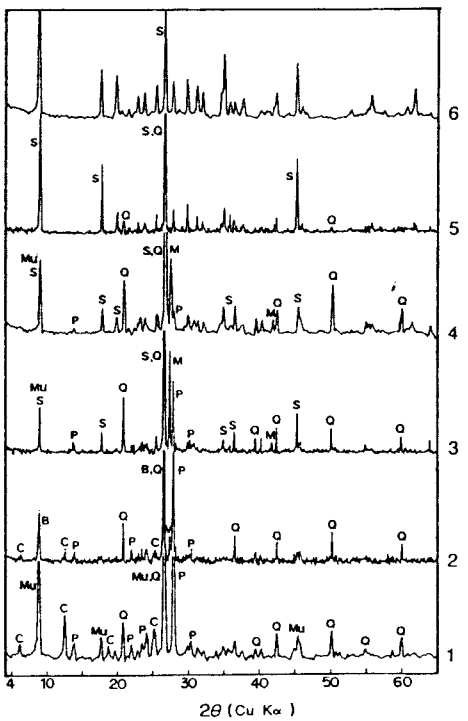


**Fig. 3.** X-ray diffraction patterns showing the gradational sericitization of the host rock (B; biotite, C; chlorite, P; plagioclase, M; microcline, Mu; muscovite, Q; quartz, S; sericite). 1, 2: Host rock, 3, 4: Moderately altered rock, 5, 6: Sericite.

## FORMATION OF SERICITE

Microscopic study shows that feldspar group minerals, albite and microcline are liable to alteration, thus changing completely to sericite, whereas plagioclase rich in Ca are often altered to albite with release of $Ca^{2+}$. The calcium liberated by albitization of plagioclase was used to form carbonate (Fig. 4A). Fig. 4B shows that the albitized plagioclase has been sericitized leaving the original plagioclase (oligoclase) unaltered, suggesting that plagioclase has been firstly albitized and subsequently sericitized.

The sericitization of feldspar is structurally controlled: sericite flakes tend to lie parallel to the crystallographic planes or cleavages of feldspar. Sericites formed from plagioclase are usually fine-grained, flaky or fibrous in morphology, whereas those from microcline are relatively coarse-grained.

Biotite is generally one of the first minerals to show the effects of ore solutions. The alteration of biotite to chlorite or muscovite is a characteristic feature of an early stage hydrothermal alteration. The alteration is commonly incomplete and sporadic even within a single thin section, suggesting that equilibrium is not normally attained during the early stage of hydrothermal alteration (Schwartz, 1958). The lenses of carbonates such as ankerite, siderite and calcite are commonly found in most altered biotite grains. The structure of biotite exerts a strong control on the alteration as shown by the occurrence of two or three minerals in band parallel to the cleavage of biotite (Fig. 5A). In general, the biotite-chlorite transformation must release considerable potassium. The released potassium forms minute particles of potassium feldspar within biotite (Fig. 5B), or

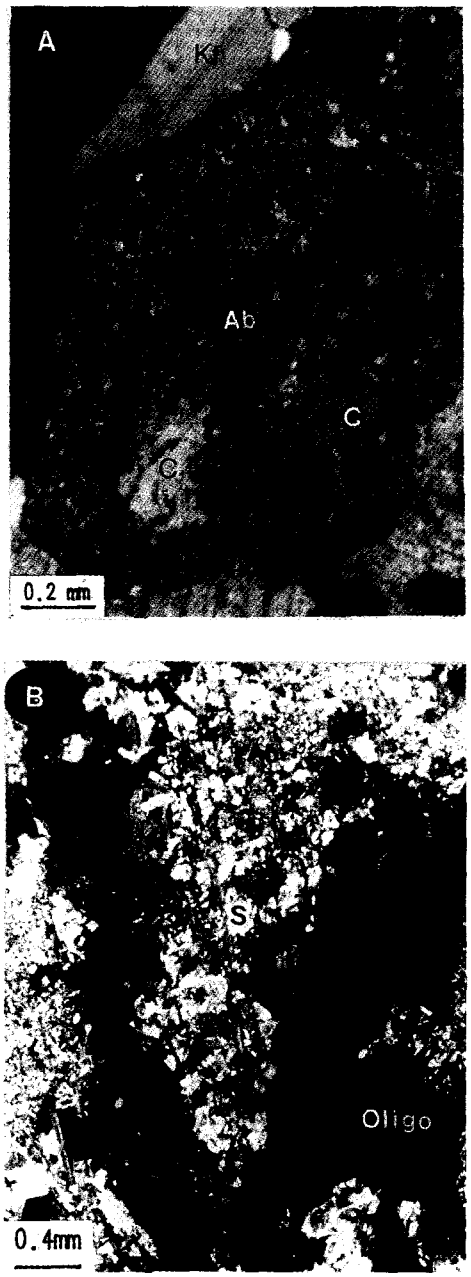


**Fig. 4.** Photomicrographs showing the sericitization of plagioclase. Oligoclase is fresh while albite has been deeply sericitized. Crossed nicols. A: Albite (Ab) and calcite (C) formed by albitization of plagioclase. B: The prior albitization of oligoclase and subsequent sericitization of albite.

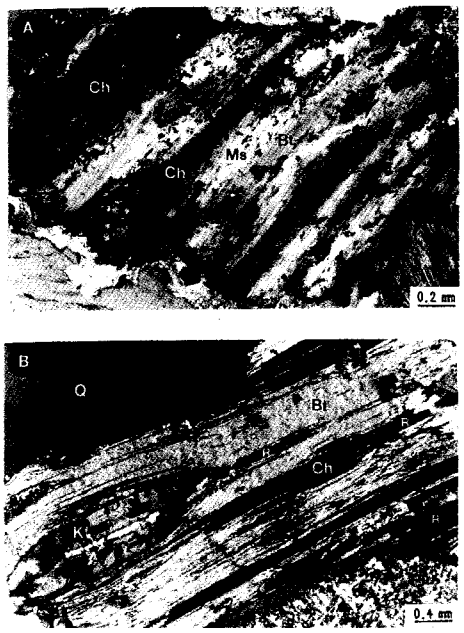


**Fig. 5.** Photomicrographs showing the transformation of biotite to chlorite and the secondary muscovite in the Hongjesa granite. A: Interleaved chlorite (Ch) and the secondary muscovite (Ms) are shown with remnant of biotite (Bt). B: Large inclusion of K-feldspar (Kf) is shown in biotite, and the dark and small inclusions of rutile(R) are precipitated along the cleavage.

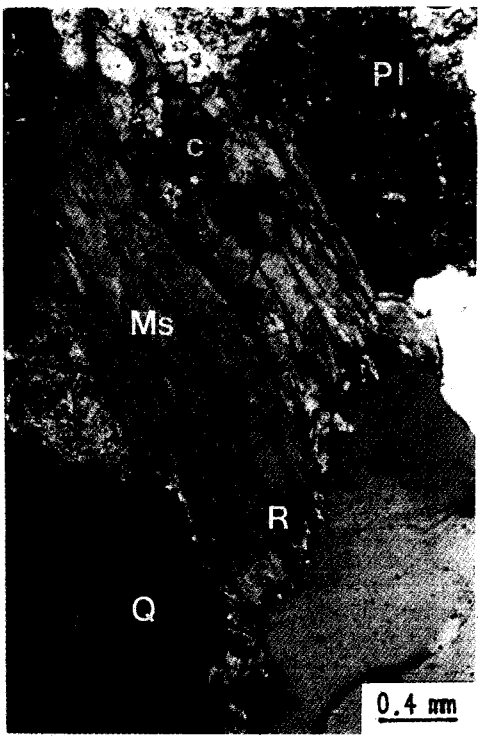


**Fig. 6.** Photomicrograph showing the muscovite pseudomorph after biotite in the alteration zone. Dark and small inclusions (rutile, R) within the secondary muscovite (Ms) indicate that biotite has been replaced by the secondary muscovite. (C; calcite). Crossed nicols.

it may have been added to the potassium feldspar already existing in the rocks (Chayes, 1955). The release of titanium has resulted in the formation of rutile (Fig. 5B).

The perfect, or nearly perfect muscovite pseudomorphs after biotite are abundant in the muscovite granite where sericitization of the rock is more intense. It is characteristic that even in the case where biotite is severely altered, its original outline is still preserved by disseminated leucoxene aggregates or rutile grains (Fig. 6). Therefore the secondary muscovite altered from biotite is easily discerned from the primary muscovite.

In the alteration of biotite, it should be emphasized that fine shreddy or flaky sericite, has been formed as the intermediate alteration product such as chlorite or the secondary muscovite. Fig. 7A shows a series of process of alteration from botite to sericite, and the remnants of chlorite are recognizable in sericite. On the other hand the primary muscovite has been directly sericitized (Fig. 7B), or sericitized through chlorite even if it is uncommon (Fig. 7C). The direct sericitization is predominantly found in the more intensely altered rock.

The formation of sericite from quartz and

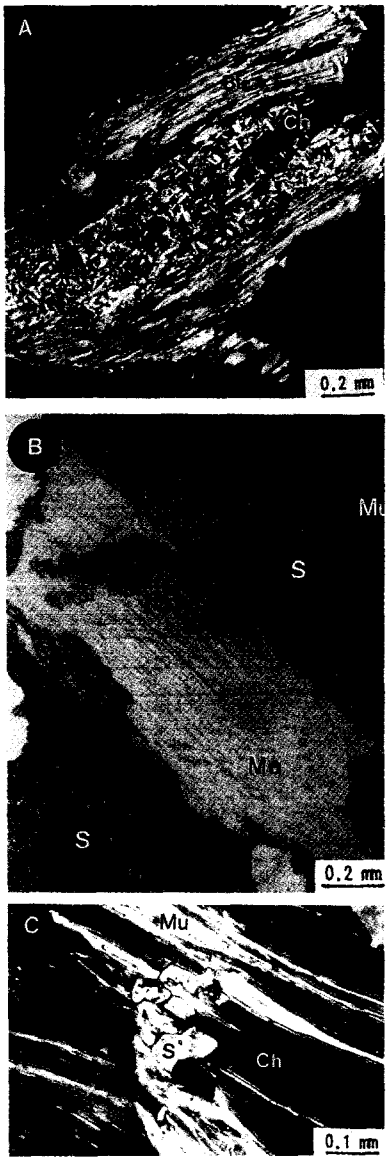


**Fig. 7.** Photomicrographs showing the sericitization of micas. Crossed nicols. A: Photomicrograph showing the formation of sericite (S) from biotite (Bt) and chlorite (Ch). Recognizable remnants of chlorite are seen in later sericite. B: Photomicrograph showing the direct sericitization from the primary muscovite (Mu). C: Photomicrograph showing the formation of sericite from the primary muscovite (Mu) and chlorite.

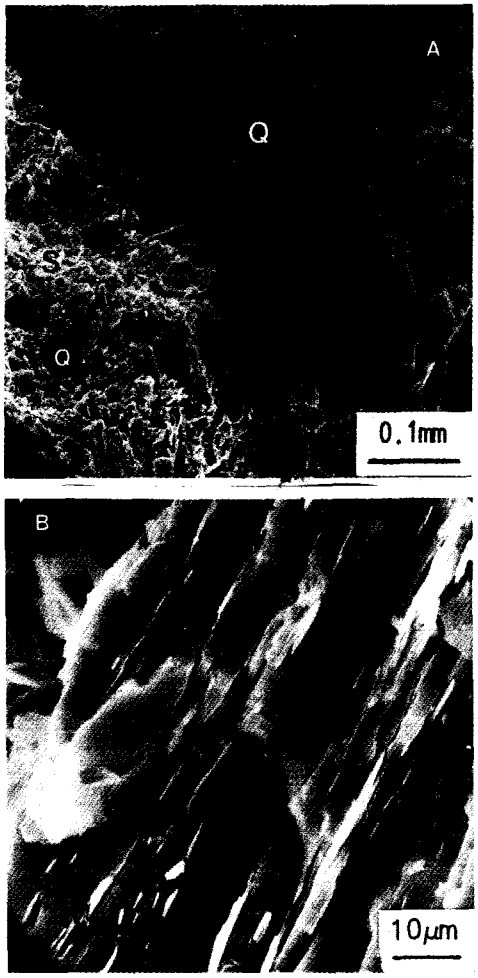


**Fig. 8.** SEM photographs showing the sericitization of quartz.

tourmaline occurred in the last stage of the hydrothermal alteration. Quartz and tourmaline, as a rule, are not well known to alter under the hydrothermal conditions. It is, therefore, very valuable to study the sericitization of these minerals.

Sericitization of quartz (Fig. 8) usually occurs along the irregular fractures or the grain boundaries, but sometimes it is found across the grain. Tourmaline is also sericitized along the irregular fractures, but it should be noted


**Fig. 9.** Photomicrographs showing the sericitization of tourmaline. A: Sericite has been directly formed from tourmaline (T). Ankerite (Ak) is an alteration product. Crossed nicols. B: Sericite has been formed from tourmaline (T) and chlorite (Ch). Note the recognizable remnants of tourmaline in later chlorite. Dark inclusions are rutile (R). Open nicol.

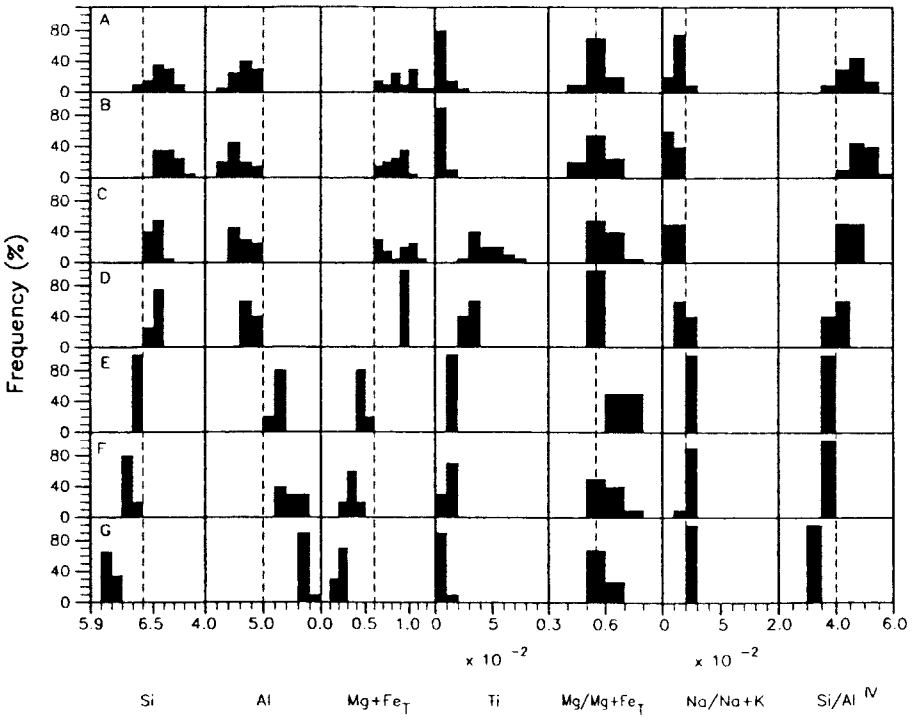


**Fig. 10.** The comparison of the chemistry of sericites of different precursors. A: Sericites formed from plagioclase. B: Sericites formed from K-feldspar. C: Sericites formed from two micas. D: Sericites formed from tourmaline and chlorite. E: Sericites directly formed from tourmaline. F: Sericites directly formed from the primary muscovite. G: Sericites formed from quartz.

that sericites have been formed through two routes : one from tourmaline (Fig. 9A), and the other from tourmaline and chlorite (Fig. 9B). The alteration products of tourmaline include sericite, chlorite, carbonates and rutile.

## CHEMISTRY OF SERICITE

Electron microprobe analyses of sericites formed from the different precursors are given in Table 4. The numerical data show the average values for 20 or more samples.

Fig. 10 represents the histogram showing the chemical differences for sericites of different precursors. As shown in this figure, sericites are divided into two groups. One is the phengitic sericite (A-D), which has been formed from feldspar, two micas and tourmaline through the secondary alteration products. And the other is the illitic sericite (E-G), which has been directly formed from the primary muscovite, quartz and tourmaline. The phengitic sericites have higher $Mg+Fe_T$ contents (>0.6) and higher $Si/Al^{IV}$ ratios (>4), but lower Na/(Na+K) ratios (<0.02) than those of the illitic sericites. $Mg/Mg+Fe_T$ ratios are rather lower (0.4~0.7) in the former than the latter. The table also shows that the composition of the precursor mineral has an influence on the composition of the later-formed sericite. For instance, sericites formed through chlorite as the intermediate alteration product have high Ti as well as high $Mg+Fe_T$ content (Fig. 10C, D), whereas sericites formed from plagioclase have slightly higher Na/(Na+K) and lower $Si/Al^{IV}$ ratios than those formed from microcline.

## POLYTYPES

X-ray diffraction pattern is used to identify

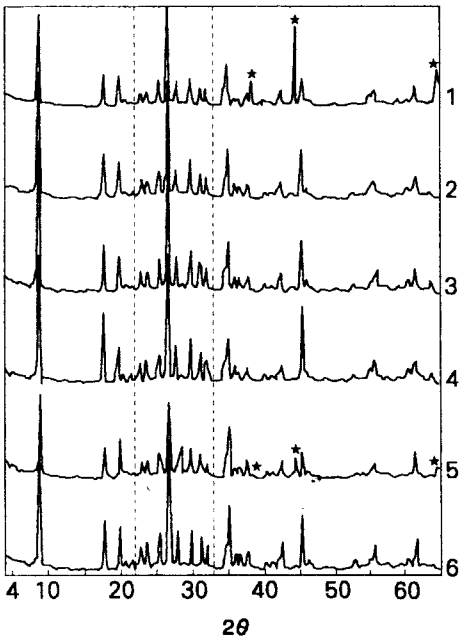


**Fig. 11.** X-ray powder diffraction patterns of sericites of $2M_1$ polytype showing different colors. (★ : tourmaline). 1. #25 (dark green), 2. #50 (green), 3. #AⅡ(yellow), 4. #2-3 (dark green), 5. #AⅣ (whitish green), 6. #E12 (yellowish green).

di, and tri-octahedral micas and polytypes (Grim, 1961; Srodon, 1984). HRTEM analysis is also useful for identification of polytypism. Both methods have been used in this study.

Sericites in the intensely altered rock are dioctahedral $2M_1$ polytype in structures, which is discerned by the peaks in the range of 22~33°($2\theta$) of the XRD patterns (Fig. 11). This figure also shows that the different colors of sericites have no relation to their structures.

Sericites in the slightly altered rock were studied using HRTEM analysis. Fig. 12 illustrates the lattice fringe image with 10Å intervals observed from the direction perpendicular to the layer plane. The selected area electron diffraction (SAED) pattern is shown in

**Table 4.** Electron microprobe analyses of sericites formed from different precursors.

| # | A | B | C | D | E | F | G |
|---|---|---|---|---|---|---|---|
| $SiO_2$ | 48.84 | 49.57 | 48.63 | 45.88 | 47.51 | 46.91 | 45.40 |
| $TiO_2$ | 0.02 | 0.00 | 0.34 | 0.72 | 0.18 | 0.13 | 0.08 |
| $Al_2O_3$ | 28.89 | 28.62 | 29.83 | 29.70 | 33.38 | 33.57 | 36.30 |
| $Cr_2O_3$ | 0.04 | 0.00 | 0.00 | 0.03 | 0.00 | 0.00 | 0.04 |
| FeO* | 2.81 | 3.27 | 2.48 | 4.04 | 1.45 | 1.07 | 0.55 |
| MgO | 2.82 | 2.71 | 2.36 | 2.49 | 1.77 | 1.53 | 0.49 |
| MnO | 0.00 | 0.03 | 0.00 | 0.08 | 0.16 | 0.07 | 0.02 |
| CaO | 0.00 | 0.02 | 0.03 | 0.03 | 0.00 | 0.00 | 0.00 |
| $Na_2O$ | 0.12 | 0.08 | 0.11 | 0.16 | 0.17 | 0.15 | 0.17 |
| $K_2O$ | 10.77 | 11.06 | 11.10 | 10.67 | 10.80 | 10.51 | 11.43 |
| Total | 94.31 | 95.36 | 94.87 | 93.78 | 95.41 | 93.93 | 94.47 |
| Numbers of ions on the basis of 22 oxygens | | | | | | | |
| Si | 6.617 | 6.662 | 6.551 | 6.327 | 6.322 | 6.314 | 6.098 |
| $Al^{IV}$ | 1.383 | 1.338 | 1.449 | 1.673 | 1.678 | 1.686 | 1.902 |
| Tet. | 8.000 | 8.000 | 8.000 | 8.000 | 8.000 | 8.000 | 8.000 |
| $Al^{VI}$ | 3.231 | 3.196 | 3.288 | 3.154 | 3.557 | 3.640 | 3.844 |
| Ti | 0.002 | 0.000 | 0.035 | 0.075 | 0.018 | 0.013 | 0.008 |
| Cr | 0.004 | 0.000 | 0.000 | 0.003 | 0.000 | 0.000 | 0.004 |
| Fe | 0.318 | 0.367 | 0.279 | 0.466 | 0.161 | 0.121 | 0.062 |
| Mg | 0.570 | 0.544 | 0.473 | 0.511 | 0.350 | 0.307 | 0.098 |
| Mn | 0.000 | 0.003 | 0.000 | 0.010 | 0.018 | 0.008 | 0.002 |
| Oct. | 4.125 | 4.109 | 4.074 | 4.219 | 4.104 | 4.088 | 4.019 |
| Ca | 0.000 | 0.003 | 0.004 | 0.004 | 0.000 | 0.000 | 0.000 |
| Na | 0.032 | 0.020 | 0.029 | 0.044 | 0.043 | 0.040 | 0.043 |
| K | 1.861 | 1.896 | 1.907 | 1.876 | 1.834 | 1.804 | 1.958 |
| Int. | 1.893 | 1.920 | 1.939 | 1.924 | 1.877 | 1.845 | 2.001 |
| Ch(Tet) | -1.38 | -1.34 | -1.45 | -1.67 | -1.68 | -1.69 | -1.90 |
| Ch(Oct) | -0.51 | -0.59 | -0.49 | -0.26 | -0.20 | -0.16 | -0.10 |
| Ch(Int) | 1.89 | 1.92 | 1.94 | 1.93 | 1.88 | 1.84 | 2.00 |
| $Si/Al^{IV}$ | 4.785 | 4.979 | 4.522 | 3.783 | 3.767 | 3.746 | 3.207 |
| Na/Na+K | 0.017 | 0.011 | 0.015 | 0.023 | 0.023 | 0.022 | 0.021 |
| Mg/Fe+Mg | 0.642 | 0.597 | 0.629 | 0.523 | 0.685 | 0.718 | 0.612 |

* Total Fe as FeO.

A : Sericites formed from plagioclase.

B : Sericites formed from K-feldspar.

C : Sericites formed from two micas through secondary muscovite or chlorite.

D : Sericites formed from tourmaline through chlorite.

E : Sericites directly formed from tourmaline.

F : Sericites directly formed from the primary muscovite.

G : Sericites formed from quartz.

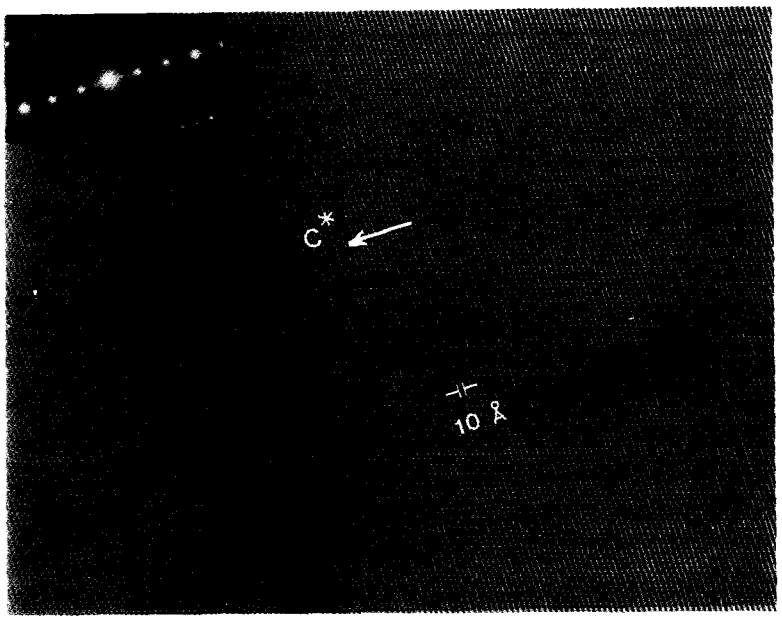


**Fig. 12.** Lattice fringe image and selected area electron diffraction (SAED) pattern of 1M sericite. Lattice fringe image shows a constant 10Å interlayer spacings.

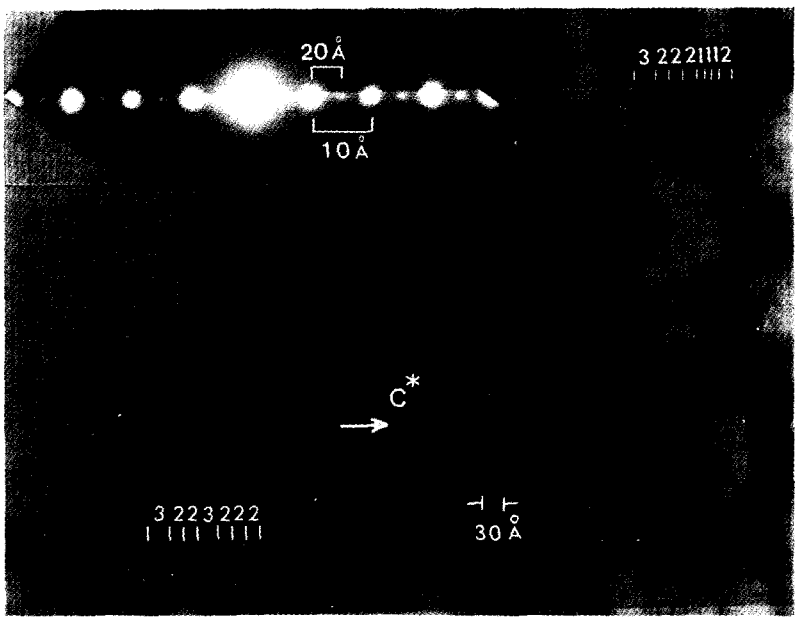


**Fig. 13.** Lattice fringe image showing irregular stacking of 1M, $2M_1$ and 3T types. The selected area electron diffraction pattern in the inset shows that the reflection from 30Å layers are so weak that they are lost in the background, owing to its low proportion.

the inset. Fig. 13 shows the lattice fringe image of randomly interlayered 1-layer (1M), 2-layer ($2M_1$) and 3-layer (3T) polytypes sericites, and this is why the electron diffraction pattern in the inset shows streaking and diffuseness along c* (Iijima et al., 1978). 3T polytype tends to coexist with $2M_1$ polytype as shown by Liborio et al. (1975), but the proportion of 30 layer is very low.

## DISCUSSION

The amount of celadonite substitution is a function of pressure and temperature, although bulk rock composition may also be significant (Ernst, 1963; Velde, 1965b, 1967; Brown, 1968; Powell and Evans, 1983).

Using the condition of hydrothermal alteration, celadonite content ($Mg+Fe_T$) and polytype, sericites from the Daehyun mine were roughly plotted on Velde's schematic diagram (Velde, 1965a). The diagram shows that sericites are classified into two genetic groups : A and B as shown in Fig. 14. Group A corresponds to sericites with less celadonite content and $2M_1$ polytype, and group B corresponds to sericites with more celadonite content and 1M polytype. As shown in this figure, it is expected that the former might be formed under the relatively high temperature (280~350℃) and low pressure, whereas the latter might be formed under the low temperature (160~280℃) and low pressure.

In summary, sericites formed from the primary muscovite, tourmaline and quartz under the relatively high temperature are of $2M_1$ polytype having less $Mg+Fe_T$ contents, whereas sericites formed from feldspar, biotite, muscovite, tourmaline and the secondary alteration products under the relatively low temperature are of 1M, $2M_1$ and 3T polytypes having more

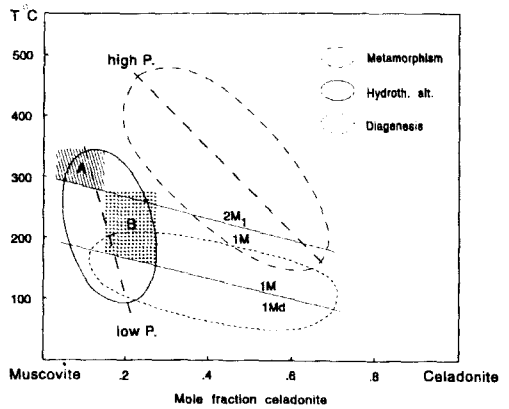


**Fig. 14.** Schematic diagram showing variations with physical conditions in chemical composition and polytype of dioctahedral potassium mica minerals (Velde, 1965a). Marking A and B represent sericites which belong to (E-G) and (A-D) group in Fig. 10, respectively.

$Mg+Fe_T$ contents. In other words, sericites having the octahedral composition closer to the primary muscovite are characterized by $2M_1$ polytype, but it changes to 1M by addition of small amounts of celadonite composition ($Mg+Fe_T$). Therefore a general sequence of 1M→ $2M_1$ transformation is expected with the increase of temperature as Yoder and Eugster (1955) and Velde (1965b) suggested.

## CONCLUSION

The Daehyun sericite deposit has been formed by the hydrothermal alteration of the Hongjesa granite, leaving the muscovite granite between ore body and the Hongjesa granite as the wall-rock alteration zone.

There are two genetic types of sericites having different chemistry and polytype: they are the early and late sericites. The early sericite of $2M_1$ polytype having octahedral

composition close to muscovite was formed from primary muscovite, tourmaline and quartz under a relatively high temperature. The late sericite of 1M, $2M_1$ and 3T polytypes having phengitic composition was formed from feldspar, biotite, muscovite and tourmaline under a relatively low temperature.

## REFERENCES


김종환, 유장한, 박용순, 김용욱 (1984) 대현 견운모광상 조사 : 비금속광상연구, 한국동력자원연구소, 99-128.

대한광업진흥공사 (1987) 비금속광물 특성조사보고서(고령토, 납석 편)

박희인, 장호완, 진명식 (1988) 태백산지역 내 광상의 생성연령. 광산지질, 21, 57-67.

양정일, 신희명, 황선국, 배광현(1996) 산업원료광물의 고부가가치 연구(운모, 장석을 중심으로). 광물학회 심포지움, "산업광물" 중에서, 한국광물학회, 74-88.

Brown, E. H. (1968) The $Si^{4+}$ content of natural phengite : A discussion. Contrib. Mineral. Petrol., 17, 78-81.

Chayes, F. (1955) Potash feldspar as a by-product of the biotite-chlorite transformation. Jour. Geol., 63, 75-82.

Ernst, W. G. (1963) Synthetic and natural muscovite. Geochim. Cosmochim., Acta, 6, 157-185.

Ernst, W. G. (1963) Significance of phengitic micas from low grade schist. Amer. Min., 48, 1357-1373.

Grim, R. E. (1968) Clay Mineralogy (2nd ed.). McGraw-Hill, New york, 126-158.

Iijima, S. and Buseck, P. R. (1978) Experimental study of disordered mica structures by high resolution electron microscopy. Acta. Crystallographica, A34, 709-719.

Kelsey, C. H. (1965) Calculation of the C.I.P.W. Norm. Mineral Mag., 34, 276-282.

Kim, D. H., Choo, S. H., and Lee, D. J. (1978) Rb/Sr age of the Hongjesa granite distributed in Seogpori area. Report Geosci. Mineral Resource, 4, 83-101.

Liborio, G. and Mottana, A. (1975) White micas with 3T polymorph from the Calcescisti of the Alps. Neues Jahrbuch für Minerogie, Monatschefte, 546-555.

Rhee, B. Y. (1991) Mineralogy of sericites in the Daehyun mine, Korea. Unpub. Ph. D. Thesis, Seoul Nat. Univ.

Robinson, P. (1984) Woodlands clay - sericite mica in a clay-like state.

Schwartz, G. M. (1958) Alteration of biotite under mesothermal conditions. Economic Geol., 53, 164-177.

Srodon, J. (1984) X-ray powder diffraction identification of illitic materials. Clay and Clay Miner., 32, 337-349.

Tokubo, K. (1986) Application of powders to cosmetics - their properties and reform of their function. Fragrance Jour., No. 80, 60-66.

Velde, B. (1965a) Phengite micas : Synthesis, stability and natural occurrence. Amer. Jour. Sci. 263, 886-913.

Velde, B. (1965b) Experimental determination of muscovite polymorph stabilities. Amer. Miner., 50, 436-449.

Yoder, H. S. and Eugster, H. P. (1955) Synthetic and natural muscovites. Geochim. Cosmochim. Acta, 7, 225-280.